

ECG Changes After Rabbit Coronavirus Infection

Lorraine K. Alexander, DRPH,* Bruce W. Keene, DVM,†
Boyd L. Yount, BS,* Joachim Dieter Geratz, MD,‡
J. David Small, DVM, MPH,* and Ralph S. Baric, PhD*

Abstract: This study examines the electrocardiographic (ECG) changes following rabbit coronavirus (RbCV) infection. We have shown that infection with RbCV results in the development of myocarditis and congestive heart failure and that some survivors of RbCV infection go on to develop dilated cardiomyopathy in the chronic phase. Serial ECGs were recorded on 31 RbCV-infected rabbits. Measurements of heart rate; P-R interval; QRS duration; QTc interval; and P-, QRS-, and T-wave voltages were taken. The recordings were also examined for disturbances of conduction, rhythm, and repolarization. The acute and subacute phases were characterized by sinus tachycardia with depressed R- and T-wave voltages as well as disturbances of conduction, rhythm, and repolarization. In most animals in the chronic phase, the sinus rate returned to near-baseline values with resolution of the QRS voltage changes. The ECG changes observed during RbCV infection are similar to the spectrum of interval/segment abnormalities, rhythm disturbances, conduction defects, and myocardial pathology seen in human myocarditis, heart failure, and dilated cardiomyopathy. Because animals often died suddenly in the absence of severe clinical signs of congestive heart failure during the acute phase, RbCV infection may increase ventricular vulnerability, resulting in sudden cardiac death. RbCV infection may provide a rare opportunity to study sudden cardiac death in an animal model in which the ventricle is capable of supporting ventricular fibrillation, and invasive techniques monitoring cardiac function can be performed. **Key words:** coronavirus, myocarditis, heart failure, ECG.

*From the * Department of Epidemiology, School of Public Health, ‡ Department of Pathology, School of Medicine, The University of North Carolina at Chapel Hill, Chapel Hill, NC; and the † College of Veterinary Medicine, North Carolina State University, Raleigh, NC.*

Supported by grants from the American Heart Association, 90112, the National Institutes of Health, AI23946, and a fellowship from the American Heart Association, North Carolina Affiliate, NC-93-FW-01, to LKA. This work was performed during an Established Investigator Award from the American Heart Association, 890193, to RSB.

Reprint requests: Ralph S. Baric, PhD, Department of Epidemiology, School of Public Health, The University of North Carolina at Chapel Hill, Chapel Hill, NC 27599-7400.

Copyright © 1999 by Churchill Livingstone®

0022-0736/99/3201-0004\$10.00/0

Viral infection of the heart can lead to myocarditis, dilated cardiomyopathy, progressive heart failure, and sudden cardiac death (1,2). Myocarditis is thought to develop in approximately 2 to 5% of patients following acute viral infection (3,4). The diagnosis of viral myocarditis is problematic due to the lack of definitive clinical signs and the paucity of sensitive diagnostic tests (1). Diagnosis can be further complicated by the variable time course of progression of viral myocarditis, with clinically unapparent viral infection (even early in childhood), potentially resulting in dilated cardiomyopathy weeks, months, or even years later (5). Rapidly accumulating evidence based on nucleic acid hybridization and other molecular techniques supports the hypothesis that cardiotropic viruses play an important role in the pathogenesis of myocarditis and dilated cardiomyopathy (6–10). Difficulties inherent in diagnosing and studying the pathogenesis of viral myocarditis have prevented an accurate assessment of the prevalence of virus-induced heart disease in the human population.

Animal models of viral myocarditis offer a valuable opportunity to study the complex interactions between virus and host with respect to both viral infection and the pathogenesis of virus-induced myocarditis and dilated cardiomyopathy. An appropriate animal model could provide useful clinical diagnostic markers for the disease and serve as a model for potential therapeutic intervention once the natural history of the infection is known. A good model should induce a reproducible spectrum of disease clinically similar to that observed in humans. Recently, our laboratory has described a model of viral myocarditis, congestive heart failure (CHF), and dilated cardiomyopathy in rabbits infected with rabbit coronavirus (RbCV). The RbCV model of myocarditis and dilated cardiomyopathy has been divided into acute, subacute, and chronic phases based on duration of survival after infection, clinical signs, and pathologic findings (11–13). Survivors of RbCV infection (chronic phase) have been further categorized into those exhibiting slight myocyte hypertrophy and those with moderate hypertrophy based on myocyte diameter measurements (13). The mechanism of death after infection is unclear, especially early in infection.

Electrocardiographic (ECG) changes associated with viral infection of the heart have been studied in animal models, primarily coxsackie B and encephalomyocarditis viruses in mice (14–17), although the effects of western equine encephalitis virus, influenza A virus, and pseudorabies virus infections in the heart have also been described (18–20). In an effort to further evaluate and char-

acterize the RbCV model system, this study was designed to describe the ECG and pathologic changes associated with RbCV infection.

Methods

Animals and Viral Infection

Pathogen-free male New Zealand White rabbits (*Oryctolagus cuniculus*) (2.5 to 3.0 kg) were purchased from a commercial supplier (Robinson Services, Winston-Salem, North Carolina). All RbCV-infected rabbits were housed singly in biohazard containment cubicles at room temperature (21 to 24°C), given tap water ad libitum, and fed 150 g/day of a commercial rabbit diet (Agway, Grandville Milling, Creedmoor, North Carolina). Control rabbits were housed singly in a room separate from the infected rabbits. Thirty-one animals were inoculated intramuscularly with 0.2 mL of a RbCV stock containing 10^3 to 10^4 rabbit infectious dose/mL and observed daily for clinical signs of infection as previously described (12,13).

This study was approved by the Institutional Animal Care and Use Committee and was conducted in accordance with The Guide for Care and Use of Laboratory Animals (U.S. Department of Health and Human Services, NIH 86-23, revised 1985) and the guiding principles of the American Physiological Society. The University of North Carolina Animal Facility is fully accredited by the American Association of Laboratory Animal Care.

Pathologic and Morphometric Studies

Moribund animals (acute and subacute phases), survivors of RbCV infection (chronic phase), and uninfected controls were euthanized as previously described (12,13). The hearts, lungs, and livers of all animals were removed, weighed, and fixed in 10% phosphate-buffered formalin and processed as previously described (11,12,13). In addition, the atrioventricular (AV) node was evaluated by examining sections cut in a plane parallel and slightly distal to the base of the ventricles. These sections included the right and left ventricular free walls as well as portions of the muscular and membranous areas of the interventricular wall (21). Sections containing the AV node were stained with hematoxylin–eosin and the periodic acid Schiff stain. All histopathologic studies were performed by three investigators (LKA, JDG, DS) blinded to the animal's experimen-

tal group or phase of infection. Morphometric measurements of the ventricular areas and wall thickness of the hearts of all animals were performed as previously described (13). Myocyte fiber diameters of all rabbits in the chronic group were measured as previously described (13).

ECG Studies

Serial ECGs were performed on 31 rabbits infected with RbCV and on six uninfected controls. ECGs were recorded using a direct ink recorder (Grass model 7B, Grass Instrument Company, Quincy, Massachusetts). Surface electrodes were preamplified by an alternating current-coupled ECG preamplifier (Grass model 7P4G) and a companion pen-driven direct current driver amplifier (Grass model 7DAG). Alternatively a three-channel microcomputer-augmented cardiograph I digital transmitter/recording unit (Marquette Electronics Inc., Milwaukee, Wisconsin) was used. With the Grass polygraph, leads I, II, III, V_1 , V_2 , V_4 , and V_6 were recorded at 50 mm/s with the recorder calibrated to 1.0 mV/20 mm. With the microcomputer-augmented cardiograph I, leads I, II, III, aVR, aVL, aVF, V_1 , V_2 , V_4 , and V_6 were recorded at both 25 and 50 mm/s, with the recorder calibrated to 1.0 mV/10 mm.

Unanesthetized rabbits (infected and controls) were held in an upright, slightly elevated position while ECGs were taken. All rabbits were acclimated to the recording procedure by collecting baseline ECGs daily for 5 days prior to infection. After infection, ECGs were recorded twice daily from day 3 through 12 and then at weekly intervals through day 30 on all animals surviving infection. Five chronically infected animals were observed through day 70 postinfection, and three surviving animals were observed through days 83, 97, 120, 130, 160, and 200 postinfection. ECGs were recorded on control rabbits through day 200 at the same intervals as infected animals.

ECG parameters measured included heart rate; PR interval; QRS duration; QT interval; and P-, QRS- and T-wave voltages. All measurements were made in lead II by two investigators (LKA, BLY) blinded to the animal's experimental group or phase of infection, and a mean of four sinus-conducted beats was reported. The QT interval was corrected (QTc) for heart rate using three previously described methods. To assess whether the formulae commonly used to correct QT interval in humans and other species might be appropriately applied to rabbits, we plotted QTc as calculated by

Bazett's formula [$QTc = QT / \sqrt{[RR]}$] (22), by Van de Water et al.'s formula [$QTc = QT - 87 (60/HR - 1)$] (23), and the by the formula of Fredericia [$QTc = QT / (\sqrt[3]{RR})$] (24) against the RR intervals from normal rabbits over the range of heart rates available (160 to 300 by increments of 10 beats/min, 150 sets of RR vs. QTc intervals total; QTc = corrected QT interval, QT = QT interval, RR = RR interval, and HR = heart rate). In the rabbit, the various regression-corrected QTc values are more useful than the uncorrected data, although Bazett's formula is also of some value for correcting changes based on heart rate (25). We subsequently utilized the correction formula resulting in the flattest slope (Van de Water) to assess the effect of infection on the QT interval, and verified the effect of infection by comparing QT intervals measured at similar heart rates before and after infection. In addition, ECG recordings were examined for disturbances of conduction, rhythm, and repolarization. All ECGs were interpreted by an investigator (BWK) not present at their recording and blinded to the animal's experimental group or phase of infection.

Statistical Analysis

ECG measurements are presented as mean \pm standard deviation (for continuous variables; for discrete variables, number affected/percent affected). Differences between baseline ECG measurements and those made during the course of infection were identified by a paired *t*-test (26). Comparisons of ECG parameters measured in animals that developed chronic myocarditis (survival >12 days postinfection) with moderate versus slight myocyte hypertrophy were made by a two-sample *t*-test (26). A one-way analysis of variance was used to evaluate the statistical significance of differences in ECG measurements among the acute, subacute, and chronic groups.

Results

Mortality and Course of RbCV Infection

Of the 31 rabbits inoculated with RbCV stock, 10 (32%) died during the acute phase (days 2–5), and 7 (23%) died during the subacute phase (days 6–12) of infection. Fourteen animals (45%) survived into the chronic phase of infection and were euthanized and necropsied. Animals that died during the acute phase of infection often did so sud-

denly, without showing severe or moderate signs of heart failure. Clinical signs consistent with CHF (weakness, dyspnea, anorexia) were present in all animals that died during the subacute phase. All animals surviving into the chronic phase of infection were clinically asymptomatic at the time of euthanasia.

Pathologic Findings

Gross and microscopic findings in animals dying during the acute and subacute phases or sacrificed during the chronic phase were similar to those previously described (11,12,13).

The AV node was available for examination in five of the rabbits that died during the acute phase and four rabbits that died in the subacute phase. All of the AV nodes examined had evidence of edema

and contained small to moderate numbers of macrophages and Anitschkow cells, and rarely a few heterophils—findings not present in any of the six control rabbits. Alteration of cellular architecture of the AV nodal tissue was always minimal, despite extensive degeneration in the adjacent myocardium (Fig. 1A–D). The AV nodes of six rabbits euthanized during the chronic phase were available for examination. All were unremarkable except for the presence of a few scattered lymphocytes.

Morphometric Analysis

Ventricular area and wall thickness measurements in animals during each phase of infection were consistent with earlier studies (12,13). Morphometric analysis of the hearts of animals surviving into the chronic phase of infection revealed

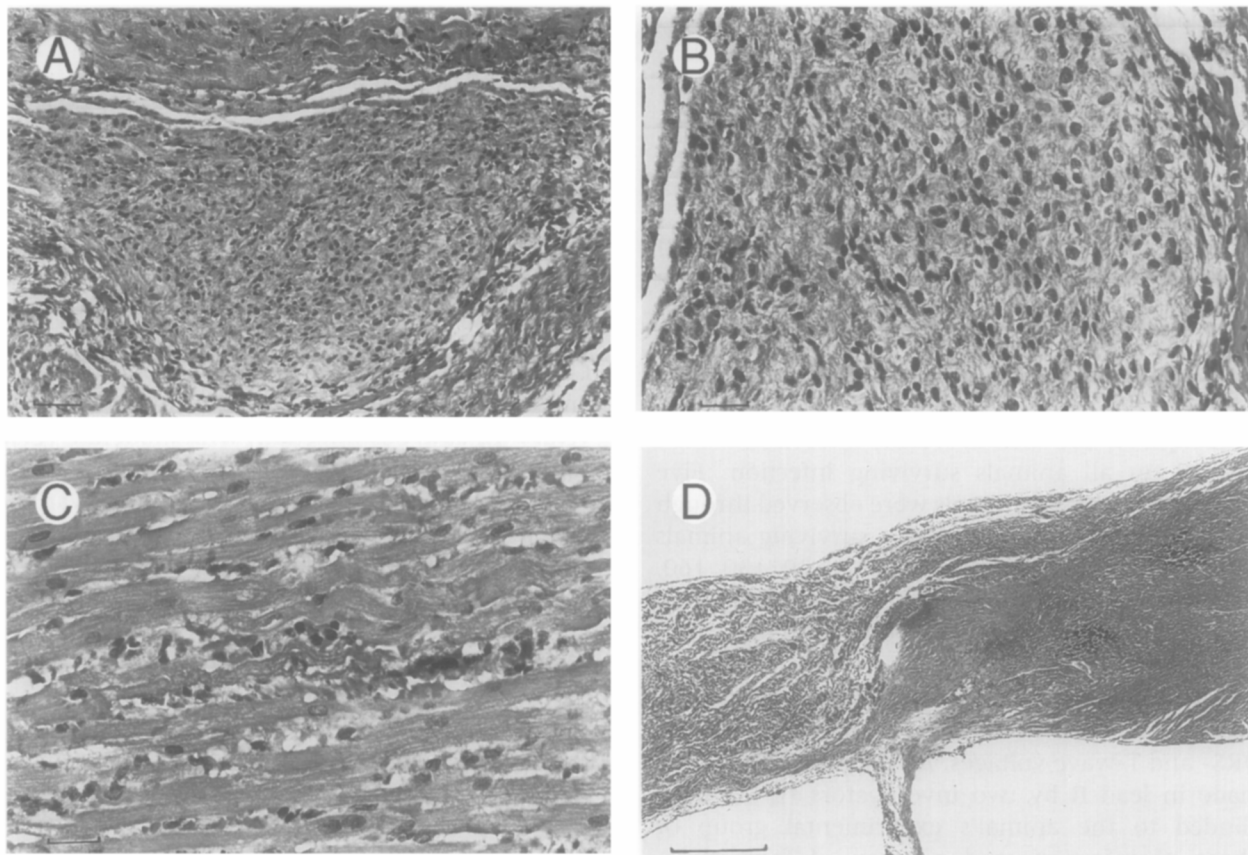


Fig. 1. Histologic changes in the AV node and in the surrounding myocardium following rabbit coronavirus infection. (A) AV node on day 6 with infiltrate of histocytes and edema. Bar = 50 μ m. (B) A high-power view of panel A. Bar = 25 μ m. (C) Myocardium adjacent to AV node on day 6 as shown in panels A and B. Focal necrosis of myocytes with interstitial edema, histocytes, and heterophils. Bar = 25 μ m. (D) The junction of the muscular and membranous portions of the interventricular septum in the vicinity of the AV node and His bundle on day 12. The myocardium has increased cellularity characterized predominantly by lymphocytes. The myocardium also contains two foci of necrosis and mineralization. Bar = 500 μ m. All sections were stained with hematoxylin–eosin. AV, atrioventricular.

Table 1. Mean Baseline Electrocardiographic Measurements From 31 Infected Rabbits and 6 Control Rabbits

PR interval*	.066 ± .007† (.056–.08)‡
QRS interval	.036 ± .007 (.02–.05)
QT interval	.139 ± .011 (.12–.16)
QTc interval§	.273 ± .022 (.23–.32)
QTc interval¶	.190 ± .012 (.17–.24)
P voltage	.098 ± .034 (.04–.18)
QRS voltage	.388 ± .10 (.22–.60)
T voltage	.252 ± .096 (.10–.50)

* Duration in seconds.

† Mean ± SD.

‡ Range of measurements.

§ QT interval corrected for heart rate using Bazett's formula ($QTc = QT / \sqrt{RR}$) (22).¶ QT interval correction proposed by Van de Water et al. [$QTc = QT - 87 (60/HR - 1)$] (23).

|| Voltage in mV.

myocyte hypertrophy, characterized as slight ($18.8 \pm 0.75 \mu\text{m}$, $n = 9$) or moderate ($22.6 \pm 1.7 \mu\text{m}$, $n = 5$) as described previously (13). No animals had severe myocyte hypertrophy ($>26 \mu\text{m}$) in this study.

Baseline and Control ECG Findings

ECGs recorded prior to infection in the 31 rabbits and in 6 control animals (days 0–200) demonstrated normal sinus rhythm with a mean heart rate of 232 ± 24 and 216 ± 18 beats/min, respectively. No significant differences were found between the two groups, and no disturbances of rhythm or conduction were observed in either group of animals. The baseline ECG parameters (Table 1) mea-

sured were consistent with previously reported values (22,27,28).

To assess whether the formulae commonly used to correct QT interval in humans and other species might be appropriately applied to rabbits, we plotted QTc as calculated by Bazetts, Fredericia, and Van de Water versus RR intervals from normal rabbits over a wide range of heart rates to determine the effect of heart rate (RR interval) on QT interval (Table 2). To assess the correction of the QT interval at various heart rates, we also plotted the QTc by the various methods versus RR interval and constructed a linear regression line through the points. Over the range of heart rates available in normal rabbits, the Van de Water formula appeared superior to Bazett's or Fredericia's in correcting the QT interval, and the slope of the Van de Water line was closest to 0 (data not shown).

To verify that the QT interval did indeed prolong during RbCV infection and that this finding was not an artifact caused by inappropriate QT correction, QT intervals measured during periods of similar heart rates before (QTb, HRb) and after (QTa, HRa) RbCV infection were compared where available using the paired *t*-test. In nearly every instance in which such comparisons were available before and after infection in an individual animal, the QT was longer at a given heart rate postinfection ($P < .001$ by one-tail, paired *t*-test) (Table 3).

ECG Findings in the Acute Phase

The acute phase of RbCV infection ($n = 31$) was characterized by sinus tachycardia in 74% of the animals, with the fastest mean heart rates recorded on day 3 postinfection (277 ± 32 beats/min, $P < .001$ vs baseline). R-wave voltages were slightly depressed throughout the acute phase in 16% of the animals, reaching their nadir on day 3

Table 2. QT Interval Correction in Rabbits

HR Range	N(Obs)*	AVG QT†	AVG HR	VdeW‡	Bazett¶	Fredericia
<200	92	138.35	176.70	195.64	237.25	198.18
200–220	78	133.88	204.18	195.88	246.88	201.32
220–240	114	135.74	225.75	199.61	263.27	211.10
240–260	66	133.08	244.62	198.73	268.65	212.56
260–280	44	126.74	263.72	193.94	265.70	207.60

* Number of observations.

† in milliseconds.

‡ Using van de Water et al. method (23).

¶ Using Bazett method (22).

|| Using Fredericia method (24).

Table 3. QT Interval Prolongation Associated With Rabbit Coronavirus Infection

Animal Number	QTb†	HRb†	HRb/QTb†	QTp‡	HRp‡	HRp/QTp‡	(HRb/QTb)–(HRp/QT)
41	140	290	2.07	130	290	2.23	–0.16
A59	110	260	2.36	110	260	2.36	0.00
1304	100	260	2.60	140	260	1.86	0.74
A56	130	250	1.92	160	250	1.56	0.36
62	160	200	1.25	160	200	1.25	0.00
X83	140	280	2.00	150	280	1.87	0.13
1293	110	220	2.00	140	220	1.57	0.43
1301	120	280	2.33	130	280	2.15	0.18
1301*	150	200	1.33	170	200	1.18	0.16
1302	120	320	2.67	130	320	2.46	0.21
1302*	130	260	2.00	140	260	1.86	0.14
14	120	260	2.17	150	260	1.73	0.43
14*	140	240	1.71	140	240	1.71	0.00
14*	130	220	1.69	140	220	1.57	0.12
21	150	200	1.33	160	200	1.25	0.08
53	140	200	1.43	150	200	1.33	0.10
53*	140	230	1.64	150	230	1.53	0.11
71	150	260	1.73	170	260	1.53	0.20
84	150	190	1.27	150	190	1.27	0.00
X88	150	240	1.60	160	240	1.50	0.10
1299	130	210	1.62	160	210	1.31	0.30
1300	150	240	1.60	150	240	1.60	0.00
1300*	150	220	1.47	160	220	1.38	0.09

* Measurements at different times/days.

† Measurements taken prior to infection and QT values are in milliseconds.

‡ Measurements taken postinfection and QT values are in milliseconds.

postinfection (mean R-wave voltage = $0.28 \pm .09$ mV, $P < .001$ vs baseline) (Figs. 2, 3). T-wave voltages were reduced throughout the acute phase in 45% of the rabbits, with the lowest mean voltage (0.11 ± 0.12 mV) recorded on day 5 postinfection, ($P < .001$ vs baseline). Other abnormalities observed during the acute phase included: QTc prolongation (32 to 42%), low-grade Mobitz type II 2° AV block (13%), ventricular premature complexes (10%), electrical alternans (10%), right bundle branch block (7%), supraventricular premature complexes (7%), and 1° AV block (3%) (Table 4, Fig. 4). Occasional ventricular premature complexes were observed in two animals with borderline QTc prolongation.

Among those animals that died in the acute phase of infection ($n = 10$), ECG abnormalities also included sinus tachycardia (70%) and decreased voltage of T waves (40%). Right bundle branch block and ventricular premature complexes were detected in two animals each prior to death (20%). ST-segment depression, QRS prolongation, and QTc prolongation were detected in one animal each (10%) prior to death during the acute phase. There were no significant differences identified between ECG parameters measured in animals dying in the acute phase and those animals surviving into the subacute and chronic phases.

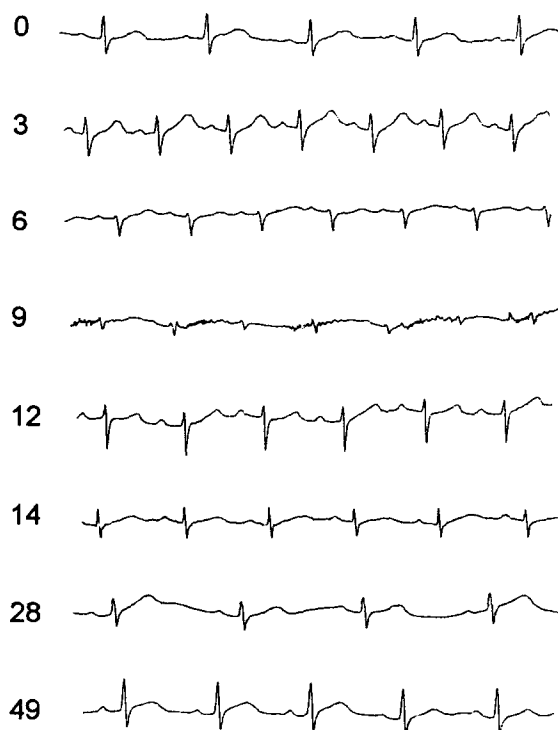
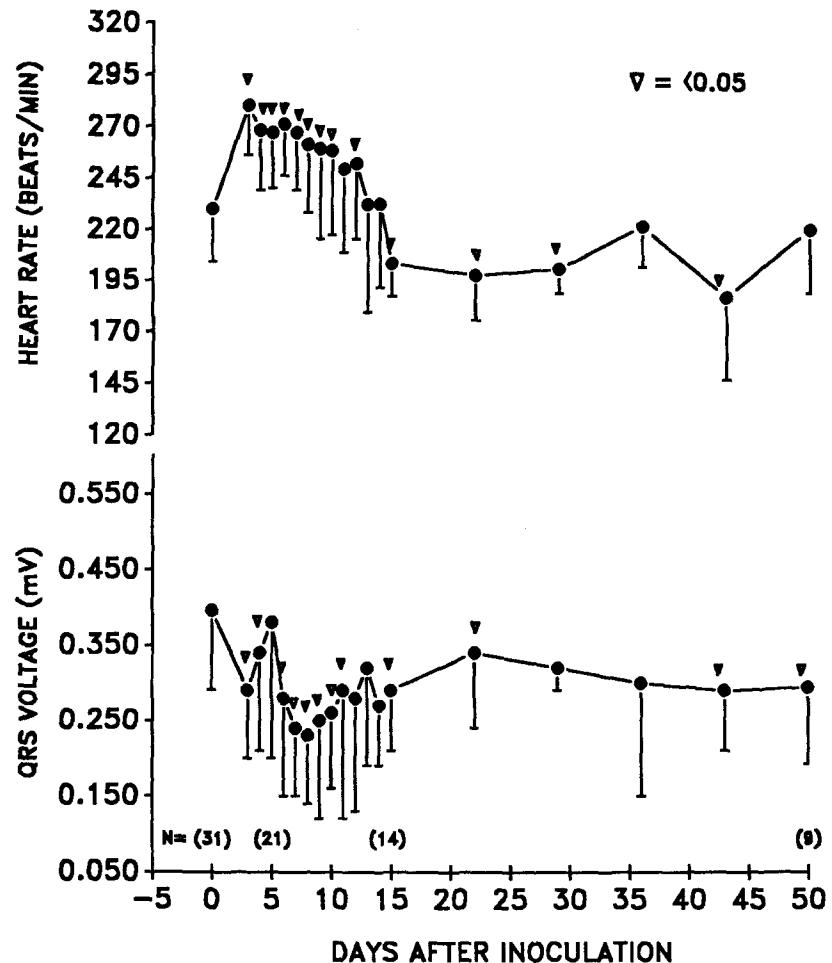
DAY

Fig. 2. Baseline (day 0) and serial electrocardiograms of a rabbit infected with rabbit coronavirus between days 0 and 49. All recordings shown are in lead II. 50 mm/sec, 1 mV = 10 mm.

Fig. 3. Mean QRS voltage and heart rate versus day of infection for 31 rabbit coronavirus-infected rabbits. Numbers in parenthesis are the number of animals surviving at that time point. Measurements were made in lead II.



ECG Findings in the Subacute Phase

The subacute phase ($n = 21$) was marked by persistent sinus tachycardia in 90% of the animals, with the highest mean heart rate recorded on day 6 after infection (271 ± 24 beats/min vs baseline, $P < .001$). During the subacute phase, the mean heart rate decreased slowly in animals that survived, returning to baseline by day 13 (232 ± 53 beats/min) for most animals. Mean R-wave voltage decreased significantly during the subacute phase (62%) with the mean low voltage (0.23 ± 0.1 mV, $P < .001$ vs baseline) occurring on day 8 postinfection. After day 8, the mean voltage began to rise, and by day 13 had returned to near normal (0.32 ± 0.13 mV) for most animals (Figs. 2, 3). T-wave voltages were also reduced in 95% of the animals and generally paralleled the R-wave voltage changes during the subacute phase. The lowest T-wave mean voltage occurred on day 7 after infection (0.08 ± 0.07 mV vs baseline, $P < .001$). Many animals in the subacute phase of infection

had prolongation of the QTc interval (43% to 89%), QRS duration (29%), and PR interval (29%). Occasional supraventricular tachyarrhythmias (10%) were seen and 2° AV block (19%) persisted in two animals and developed in two others, while one animal displayed isolated ventricular depolarizations (5%) (Table 4, Fig. 4).

Among animals that died in the subacute phase of infection ($n = 7$), ECG changes consisted of sinus tachycardia (71%), decreased voltage of T waves (86%), 1° AV block (29%), 2° AV block (29%), decreased voltage of R waves (29%), and electrical alternans (14%). There were no significant differences between ECG parameters measured in animals that died in the subacute phase and those animals that survived.

ECG Findings in the Chronic Phase

The chronic phase ($n = 14$) was characterized by the return of the sinus rate to near-baseline values

Table 4. Electrocardiographic Changes in 31 Rabbits After Infection With Rabbit Coronavirus

Electrocardiographic Changes	Acute (2–5 days) n = 31*	Subacute (6–12 days) n = 21*	Chronic (13–200 days) n = 14*
Interval/segment abnormalities			
QRS prolongation†	4 (13%)	6 (29%)	2 (14%)
QTc prolongation‡	10 (32%)	9 (43%)	4 (29%)
QTc prolongation§	15 (42%)	17 (89%)	11 (80%)
ST segment			
Elevation	1 (3%)	0 (0%)	3 (21%)
Depression	4 (13%)	0 (0%)	0 (0%)
T wave depression	14 (45%)	20 (95%)	8 (57%)
R wave depression	5 (16%)	13 (62%)	7 (50%)
Electrical alternans	3 (10%)	3 (14%)	0 (0%)
Rhythm disturbances			
Ventricular premature complexes	3 (10%)	1 (5%)	1 (7%)
Supraventricular premature complexes	2 (7%)	2 (10%)	2 (14%)
Sinus arrhythmia	0 (0%)	0 (0%)	4 (29%)
Sinus tachycardia	23 (74%)	19 (90%)	7 (50%)
Conduction defects			
1° AV block¶	1 (3%)	6 (29%)	5 (36%)
2° AV block (Mobitz type II)	4 (13%)	4 (19%)	1 (7%)
Right bundle branch block	2 (7%)	0 (0%)	0 (0%)

* Number of animals at beginning of each phase.

† Interval is increased above each animals baseline measurement; typically 0.036 sec.

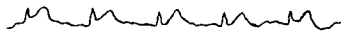
‡ Interval is >0.32 s as calculated by Bazett's formula [$QTc = QT/\sqrt{RR}$].

¶ PR interval is >0.08 s.

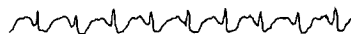
§ Two SD above the baseline QTc interval as calculated proposed by Van de Water et al. [$QTc = QT - 87 (60/HR - 1) (23)$].

AV, atrioventricular.

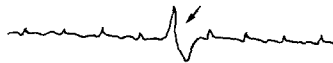
- ST SEGMENT ELEVATION, LEAD II, DAY 32



- SEGMENT DEPRESSION, LEAD I, DAY 4



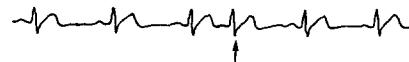
- VENTRICULAR PREMATURE COMPLEX (†), LEAD I, DAY 11



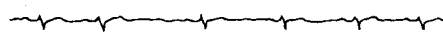
- RIGHT BUNDLE BRANCH BLOCK, LEAD I, DAY 3



- SUPRAVENTRICULAR PREMATURE COMPLEX (‡), LEAD V2, DAY 15



- SINUS ARRHYTHMIA, LEAD V2, DAY 14



- 2° AV BLOCK-TYPE II MOBILTZ, LEAD V2, DAY 13 († = P WAVE, ○ = R WAVE)

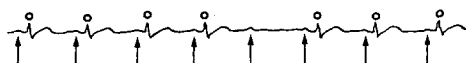


Fig. 4. ECG changes seen in rabbit coronavirus-infected rabbits. 50 mm/sec, 1 mV = 10 mm.

in 57% of the animals and resolution of QRS voltage changes by day 30 for half of the animals (Figs. 2, 3). Between days 13 and 30 postinfection ($n = 14$), ST-segment elevation (14%), PR (36%) and QTc (29 to 80%) interval prolongation, and T-wave changes (57%) occurred in some animals, and supraventricular premature complexes and 2° AV block were seen in one animal (7%). During this period, sinus arrhythmia developed in four animals (29%) (Table 4, Fig. 4). After day 30 ($n = 14$), sinus arrhythmia, 1° AV block, and decreased voltage of T waves were no longer seen, but sinus tachycardia (21%), ST-segment elevation (14%), and decreased voltage of R waves (14%) still persisted in a few animals. During this period, prolongation of the QTc interval in one animal was associated with ventricular premature complexes. No significant ECG differences were identified between animals with slight or moderate myocyte hypertrophy.

Discussion

ECG Findings in the Acute Phase

ECG observations (sinus tachycardia, QRS and decreased voltage of T waves, ST-segment changes, and ventricular and occasional supraventricular ec-

topic beats) during the acute phase of RbCV infection were generally compatible with the observed cardiac pathology in animals that died during this phase and consonant with the onset of myocarditis and early signs of heart failure. The ECG picture of acute RbCV infection mimics the spectrum of ECG abnormalities that may accompany myocarditis in humans (29–31) and is in contrast to findings in mouse encephalomyocarditis virus, where 38% of the mice dying early in the course of infection had complete AV block associated with damage to the His bundle (15).

In RbCV infection, degeneration and necrosis of myocytes as well as infiltration of the conduction system with mononuclear cells correlated with the findings of low-grade 2° AV block, occasional ventricular premature complexes, and borderline prolongation of the QTc interval recorded in one rabbit prior to death. The appropriate method of correction of the QT interval for heart rate remains controversial. Regoezci in 1961 measured the QT interval in 11 rabbits and described dependence of the QT interval in the rabbit by the regression formula $QT = 1.005^{1.25} \sqrt{HR}$ (32). Because of the methodology by which the ECGs were recorded (with the legs bound together in lateral recumbency) and the high heart rates recorded in the study, we elected not to use this specific regression formula because of probable excessive sympathetic tone during its acquisition. Hayes et al. (25) recently examined the relationship between QT and heart rate in rabbits by six different formulas, including linear, square root, and polynomial methods, concluding that various regression-corrected QT distributions were much better than the uncorrected data, with little difference among them. They judged Bazett's formula to be of "some value." We choose to correct our data with Bazett's formula and Fredericia's formula, as well as the simple linear regression equation proposed by Van de Water et al. (23). Use of the Van de Water linear equation disclosed QTc prolongation in a greater number of infected rabbits than the Bazett correction, and resulted in a flatter regression line than either the Bazett or the Fredericia correction. These data support previous findings that linear regression equations may be more useful for QT correction for heart rate than Bazett's formula (33). In studies of encephalomyocarditis, coxsackievirus B1, and western equine encephalitis virus animal models, arrhythmias and conduction defects almost always corresponded to a myocardial or conduction system injury (14,15,18). Interestingly, most animals (7) dying in the acute phase of RbCV infection had generally small, focal myocardial lesions with right

ventricular dilatation and eccentric hypertrophy. ECG findings in three of these animals included one or more of the following: right bundle branch block, occasional isolated ventricular premature complexes, decreased voltage of T waves, and ST-segment depression, but no ECG abnormalities were recorded in the other four rabbits that died during the acute phase. It seems likely that the prevalence of arrhythmias was underestimated by the method of ECG recording employed in this study (brief, intermittent monitoring periods). Similar findings in the coxsackievirus B1 model are seen when only very small patchy myocardial lesions are present, resulting in what the investigators termed "false negative" recordings (14). No ECG abnormalities were recorded in the influenza A model, in which cardiac lesions were mild and resolved quickly (19). It is possible that lesions in the central nervous systems of the rabbits may have resulted in the arrhythmias seen, although a careful examination of the brain and spinal cord of RbCV-infected animals revealed no pathologic lesions in these tissues (11,15,34,35).

Although the mechanism of sudden death during RbCV infection is unclear, both ECG and pathologic data suggest that acute RbCV infection may increase ventricular vulnerability. Similar-appearing cardiac lesions, ventricular premature complexes, and prolongation of the QTc interval have all been associated with electrical instability leading to ventricular fibrillation and sudden death in humans (36–38). Ventricular and supraventricular premature complexes and ventricular tachycardias occasionally observed early in murine encephalomyocarditis infection have also suggested the possibility of arrhythmic death in a myocarditis model (15), and a variety of ECG findings ranging from normal to prolonged QTc intervals, ventricular arrhythmias, and nonspecific T-wave changes have been associated with sudden death from suspected human viral myocarditis (2,35,39,40). As in some cases of acute RbCV infection described here, human reports exist in which seemingly insignificant focal myocardial or conduction system lesions easily missed on standard histopathologic examination were the only evidence of cardiac damage associated with sudden death (35,36,41–45).

ECG Findings in the Subacute Phase

The most frequent ECG findings in the subacute phase of RbCV infection (T waves, QTc prolongation, and sinus tachycardia with low-voltage QRS complexes) were compatible with the findings of

myocarditis and pleural effusion. These ECG findings are comparable to the variety and type of changes seen in humans with myocarditis and heart failure as well as those observed in other animal models of myocarditis and CHF (14,15,18, 40,46–48). Taken together, the ECG and pathologic findings suggest that the primary cause of death in the subacute phase of RbCV infection was heart failure.

First and low-grade 2° AV block were also commonly seen in the subacute phase. In some animals with AV block, edema and inflammatory infiltration of the AV node and surrounding myocardium were observed. In humans, inflammatory infiltration of the conduction system is believed to be the cause of death in some cases of fatal myocarditis (43,45). It has also been suggested that electrical instability of the ventricular myocardium due to damage to the cardiac sympathetic nerves may lead to prolongation of the QTc interval, which can result in potentially fatal ventricular arrhythmias (36,38).

ECG Findings in the Chronic Phase

In most survivors of the acute and subacute phases of infection, the heart rate and QRS voltages returned to normal for most animals by day 30 after infection. This was probably due to the resolution of both the acute viral myocarditis and the resultant clinical signs of heart failure. The chronic phase of infection was characterized histopathologically by hypertrophy of the remaining cardiac myocytes and resolution of the myocardial edema, findings similar to those reported following encephalomyocarditis infection (15). Some ECG abnormalities seen during the chronic phase (decreased voltage of T waves, 1° AV block and QTc prolongation, QRS prolongation, ST-segment elevation, and supraventricular ectopy) probably reflect the ongoing, presumably chronic myocarditis observed histologically.

In the chronic group judged morphometrically to have moderate myocyte hypertrophy, the dilatation and eccentric hypertrophy of the left and right ventricle in the absence of valvular or vascular lesions suggests the development of dilated cardiomyopathy (15,39,49–51). Fibrosis, myocyte hypertrophy, and persistent myocarditis are associated with ventricular conduction delays in dilated cardiomyopathy (50), producing ECG changes similar to those observed in the chronic phase of RbCV infection. Both PR interval (1° AV block) and QRS prolongation were accompanied by microscopic myocardial fibrosis as well as the presence of per-

sistent myocarditis and myocyte hypertrophy. Despite the ECG and histopathologic abnormalities, rabbits in the chronic phase did not have clinical or gross pathologic signs of heart failure, possibly reminiscent of asymptomatic human patients with cardiomegaly and nonspecific ECG abnormalities in whom the possibility of previous acute viral myocarditis has been raised (38).

Conclusions

The ECG and pathologic findings associated with RbCV infection are consistent with changes seen in humans and are similar in many respects to other animal models of viral myocarditis. Not surprisingly, the resting ECG was a relatively insensitive and nonspecific indicator of the presence and severity of RbCV-induced myocarditis, although the ECG and pathologic findings suggest that RbCV infection may increase ventricular vulnerability. RbCV infection may provide a rare opportunity to study a reproducible model of sudden cardiac death associated with viral infection in a species large enough to easily monitor the heart rate, rhythm, and function. Continuous telemetered or ambulatory ECG monitoring will be needed to completely disclose the ECG changes associated with RbCV-induced sudden cardiac death, myocarditis, and dilated cardiomyopathy.

References

1. Woodruff JF: Viral myocarditis. *Am J Pathol* 101:427, 1980
2. Abelmann WH: Viral myocarditis and its sequelae. *Ann Rev Med* 24:145, 1973
3. Abelmann WH: Virus and the heart. *Circulation* 44:950, 1971
4. See DM, Tilles JG: Viral myocarditis. *Rev Infect Dis* 13:951, 1991
5. Leslie K, Blay R, Haisch C, Lodge A, Weller A, Huber S: Clinical and experimental aspects of viral myocarditis. *Clin Microbiol Rev* 2:191, 1989
6. Tracy S, Wiegand V, McManus B et al: Molecular approaches to enteroviral diagnosis in idiopathic cardiomyopathy and myocarditis. *J Am Coll Cardiol* 15:1688, 1990
7. Tracy S, Chapman N, McManus B, Pallansch M, Beck M, Carstens J: A molecular and serologic evaluation of enteroviral involvement in human myocarditis. *J Mol Cell Cardiol* 22:403, 1990
8. Jin O, Sole M, Butany J et al: Detection of enterovi-

- rus RNA in myocardial biopsies from patients with myocarditis and cardiomyopathy using gene amplification by polymerase chain reaction. *Circulation* 82:8, 1990
9. Klingel K, Hohenadl C, Canu A et al: Ongoing enterovirus-induced myocarditis is associated with persistent heart muscle infection: quantitative analysis of virus replication, tissue damage and inflammation. *Proc Natl Acad Sci USA* 89:314, 1992
 10. Petitjean J, Kopecka H, Freymuth F et al: Detection of enteroviruses in endomyocardial biopsy by molecular approach. *J Med Virol* 37:76, 1992
 11. Small JD, Aurelian L, Squire RA et al: Rabbit cardiomyopathy. Associated with a virus antigenically related to human coronavirus strain 229E. *Am J Pathol* 95:709, 1979
 12. Edwards S, Small JD, Geratz JD, Alexander LK, Baric RS: An experimental model for myocarditis and congestive heart failure after rabbit coronavirus infection. *J Infect Dis* 165:134, 1992
 13. Alexander LK, Small JD, Edwards S, Baric RS: An experimental model for dilated cardiomyopathy after rabbit coronavirus infection. *J Infect Dis* 166:978, 1992
 14. Hoshino T, Matsumori A, Kawai C, Imai J: Electrocardiographic abnormalities in syrian golden hamsters with coxsackievirus B1 myocarditis. *Jpn Circ J* 46:1305, 1982
 15. Kishimoto C, Matsumori A, Ohmae M, Tomioka N, Kawai C: Electrocardiographic findings in experimental myocarditis in DBA/2 mice: complete atrioventricular block in the acute stage, low voltage of the QRS complex in the subacute stage and arrhythmias in the chronic stage. *J Am Coll Cardiol* 3:1461, 1984
 16. Morita H, Kitaura Y, Deguchi H, Kotaka M, Kawamura K: Experimental coxsackie B3 virus myocarditis in golden hamsters. II. Evaluation of left ventricular function in intact in situ heart 14 months after inoculation. *Jpn Circ J* 48:1097, 1984
 17. Gwathmey JK, Nakao S, Come PC et al: An experimental model of acute and subacute viral myocarditis in the pig. *J Am Coll Cardiol* 19:864, 1992
 18. Monath TP, Kemp GE, Cropp CB, Chandler FW: Necrotizing myocarditis in mice infected with western equine encephalitis virus: clinical, electrocardiographic, and histopathologic correlations. *J Infect Dis* 138:59, 1978
 19. Kotaka M, Kitaura Y, Deguchi H, Kawamura K: Experimental influenza A virus myocarditis in mice. Light and electron microscopic, virologic, and hemodynamic study. *Am J Pathol* 136:409, 1990
 20. Olsen GR, Miller LD: Studies on the pathogenesis of heart lesions in dogs infected with pseudorabies virus. *Can J Vet Res* 50:245, 1986
 21. James TN: Anatomy of the cardiac conduction system in the rabbit. *Circ Res* 20:638, 1967
 22. Lange K, Weiner D, Gold MMA: Studies on the mechanism of cardiac injury in experimental hypothermia. *Ann Intern Med* 31:989, 1949
 23. Van de Water A, Verheyen J, Xhonneux R, Reneman RS: An improved method to correct the QT interval of the electrocardiogram for changes in heart rate. *J Pharmacol Meth* 22:207, 1989
 24. Fredericia LS: Die Systolendauer in EKG bei normalen Menschen u. bei Herzkranken. *Act Medica Scand* 53:469, 1920
 25. Hayes E, Pugsley MK, Penz WP, Adaikan G, Walker MJA: Relationship between QaT and RR intervals in rats, guinea pigs, rabbits, and primates. *J Pharmacol Toxicol Meth* 32:201, 1994
 26. Wilkinson L: SYSTAT: the system for statistics. SYSTAT, Inc., Evanston, IL, 1990
 27. Saitanov AO: The electrocardiogram of healthy rabbits in standard and chest leads and methods of recording it. Translated from Byulleten Eksperimentalnoi Biologii i Meditsiny 49:102, 1960
 28. Nelson CV, Waggoner WC, Gastonguay PR: High-fidelity electrocardiograms of normal rabbits. *Am J Physiol* 207:1107, 1964
 29. Heger JW, Roth RF, Niemann JM, Criley JM: Cardiology. Williams & Wilkins, Baltimore, MD, 1993
 30. Brooks HL: Electrocardiography: 100 diagnostic criteria. Year Book Medical Publishers, Chicago, IL, 1987
 31. Scheidt S: Basic electrocardiography: leads, axes, arrhythmias. *Clin Symp* 35:1, 1983
 32. Regoezi E: Über die Frequenzabhängigkeit der Austreibungszeit und der QT-Dauer beim Kaninchen. *Zeitschrift für die gesamte experimentelle Medizin* 135:30, 1961
 33. Hodges M, Salerno D, Erlie D: Bazett's QT correction reviewed: evidence that a linear QT correction for heart rate is better. *J Am Coll Cardiol* 1:694, 1983
 34. Levine HD: Virus myocarditis: a critique of the literature from clinical, electrocardiographic, and pathologic standpoints. *Am J Med Sci* 277:132, 1979
 35. Talman WT: Cardiovascular regulation and lesions of the central nervous system. *Ann Neurol* 18:1, 1985
 36. James TN, Froggatt P, Atkinson WJ et al: Observations on the pathophysiology of the long QT syndromes with special reference to the neuropathology of the heart. *Circulation* 57:1221, 1978
 37. Baroldi G: Pathology and mechanisms of sudden death. p. 529. In Hurst JW (ed): *The Heart*. McGraw-Hill, New York, 1986
 38. Bos I, Johannisson R, Djonlagic H: Morphologic alterations in the long Q-T syndrome. Light and electron microscopic observations in the conduction system and in sympathetic trunks. *Pathol Res Pract* 180:691, 1985
 39. Obeyesekere I, Hermon Y: Arbovirus heart disease: myocarditis and cardiomyopathy following dengue and chikungunya fever—a follow-up study. *Am Heart J* 85:186, 1973
 40. Smith WG: Coxsackie B myopericarditis in adults. *Am Heart J* 80:34, 1970
 41. James TN: Intracardiac ganglionitis and sudden death. Herpes of the heart? *Trans Am Clin Climatol Assoc* 91:177, 1979

42. Tsiplenkova VG, Pavlovich ER, Balogh I, Somogyi E, Vikhert AM: Electron microscopic demonstration of viruses and bacteria in cardiac myocytes from victims of sudden cardiac death. *Acta Morphol Hung* 34:209, 1986
43. Morales AR, Adelman S, Fine G: Varcella myocarditis. A case of sudden death. *Arch Pathol* 91:29, 1971
44. James TN, Imamura K: Virus-like particles associated with intracardiac ganglionitis in 2 cases of sudden unexpected death. *Jpn Heart J* 22:447, 1981
45. Sevy S, Kelly J, Ernst H: Fatal paroxysmal tachycardia associated with focal myocarditis of the Purkinje system in a 14-month-old girl. *J Pediatr* 72:796, 1968
46. Sareli P, Schamroth MB, Passias J, Schamroth L: Torsade de pointes due to coxsackie B3 myocarditis. *Clin Cardiol* 10:361, 1987
47. Obeyesekere I, Hermon Y: Myocarditis and cardiomyopathy after arbovirus infections (dengue and chikungunya fever). *Br Heart J* 34:821, 1972
48. Levander-Lingren M: Studies in myocarditis. I. Etiology and primary course. *Cardiologia* 45:362, 1964
49. Hamby RI, Raia F: Electrocardiographic aspects of primary myocardial disease in 60 patients. *Am Heart J* 76:316, 1968
50. Wilensky RL, Yudelman P, Cohen AI et al: Serial electrocardiographic changes in idiopathic dilated cardiomyopathy confirmed at necropsy. *Am J Cardiol* 62:276, 1988
51. Kitaura Y, Morita H: Secondary myocardial disease. Virus myocarditis and cardiomyopathy. *Jpn Circ J* 43:1017, 1979